Sorption of bismuth(III) and its chloride complexes with 2-aminopyrimidine cation on hydroxyapatite of various textures

A. V. Severin,[a] Ia. A. Berezin,[a] M. A. Orlova,[a,b★] T. P. Trofimova,[a] A. Yu. Lupatov,[c] A. V. Egorov,[a] and V. M. Pleshakov[a]

[a]*Department of Chemistry, Lomonosov Moscow State University, Build. 3, 1 Leninskie Gory, 119991 Moscow, Russian Federation. E-mail: orlova.radiochem@mail.ru*
[b]*N. I. Pirogov Russian National Research Medicinal University, 1 ul. Ostrovityanova, 117997 Moscow, Russian Federation*
[c]*V. N. Orekhovich Institute of Biomedical Chemistry, Russian Academy of Medical Sciences, Build. 8, 10 ul. Pogodinskaya, 119435 Moscow, Russian Federation*

Specific features of the interaction between bismuth(III) and hydroxyapatite (HAP) of various morphologies during its sorption and co-crystallization binding were revealed. The obtained sorption isotherms nearly coincide with each other regardless of the HAP type used and cannot be described in terms of the Langmuir or Freundlich models. Bismuth can form the intrinsic phase of bismuth phosphate due to the chemical or topochemical reaction with HAP when the sorption method is used. In the case of co-crystallization binding of bismuth ions, the morphological modification of HAP occurs. The bismuth complexes with aminopyrimidine in neutral and weakly acidic solutions are readily hydrolyzed to form a precipitate, and no binding with HAP occurs.

Key words: bismuth(III), complexes with 2-aminopyrimidine, hydroxyapatite, sorption.

The development of anticancer therapy resulted in active studies of transition metal compounds, including the possibility of modeling,[1] which significantly improved understanding of their properties. It turned out that the metal complexes can function as prodrugs, and this makes it possible to design constructions of drugs of diverse action. In addition, it has been shown[2] for cisplatin and bismuth salts that the transition metal drugs can exert a synergic effect. Bismuth is of special interest along with the potential use of its compounds in chemotherapy, since it has radionuclides important for radiation therapy: α-emitters ^{212}Bi and ^{213}Bi.[3,4]

Bismuth can form coordinately diverse structures (its coordination number varies from three to ten) and tends to hydrolysis and formation of hydroxo complexes similar to the lanthanide complexes.[5,6] Supramolecular interactions (hydrogen bonds between the chlorobismuthate(III) anion and organic cation) were found to play an important role in the stabilization of $[BiCl_6]^{3-}$ and $[Bi_2Cl_{10}]^{4-}$ anions in the compounds of ion pairs: $[C_5H_7N_2]_3[BiCl_6]$ (**1**), $[C_5H_7N_2][C_5H_8N_2][BiCl_6]$ (**2**), and $[C_{10}H_{10}N_2]_2[Bi_2Cl_{10}]$ (**3**).[7]

Compounds **1** and **2** crystallize in the triclinic crystal system ($P1$), while compound **3** crystallizes in the monoclinic crystal system ($P2_1/c$), which is characteristic of the complexes of this metal in the oxidation state +3. In this case, hydrogen bonds are a powerful stimulus for the formation of network bonds and for the stabilization of the ionic structure.[8,9] In the case of the 2-aminopyrimidinium cation (AP), two complexes with the Bi : AP ratio equal to 1 : 2 were obtained[10] (2 : 4 is the binuclear complex with the space group $P1$, $(C_4H_6N_3)_4[Bi_2Cl_{10}]$ (**4**)) and 1 : 3 (space group $P2_1$, $(C_4H_6N_3)_3[BiCl_6]$ (**5**)). It turned out that the transition of complex **4** to **5** occurred under certain conditions, *i.e.*, saturation with an organic cation with a change in the structure and crystal system. The AP cation is a basis for the synthesis of many anticancer drugs (in particular, antileukemia drugs) and, hence, its transition metal complexes and their sorption on probable supports, for instance, hydroxyapatite (HAP, general formula $Ca_{10}(PO_4)_6(OH)_2$) are important for the further use of the complex drugs in medicine. It was assumed[11] that bismuth incorporated into the HAP structure can substitute calcium in position Ca2. Even during the introduction of bismuth ions simultaneously with strontium ions bismuth can competitively substitute Ca2, whereas strontium occupies the site Ca1.[12] Note that silicon-, magnesium-, strontium-, and zinc-substituted HAP favor the fast mineralization of bones.[13] A distinctive feature of the bismuth(III) ion compared to other metal ions (Mg^{2+}, Zn^{2+}, La^{3+}, Y^{3+}, In^{3+}) is a higher capability of interacting with osteoblasts,[14], which in combination

Published in Russian in *Izvestiya Akademii Nauk. Seriya Khimicheskaya,* No. 4, pp. 0665—0670, April, 2020.
1066-5285/20/6904-0665

with HAP can probably enhance chemotherapeutical possibilities of the effect on metastases in bones. It was found[15] that various Bi concentrations in the Bi-M-HAP nanoparticles (M-HAP is mineral-substituted hydroxyapatite) inhibited (dose-dependent) the function of cancerous osteoblasts with the simultaneous stimulation of the function of healthy cells.

In addition to the co-crystallization binding method for the formation of HAP-Bi composites, the adsorption method is possible for binding bismuth cations and HAP nanoparticles. According to published data,[16] the sorption kinetics of bismuth on HAP from acidic solutions is well described by the pseudo-second-order model, whereas the sorption isotherm is described by the model similar to the Langmuir model with the maximum sorption at a level of $3 \cdot 10^3$ (mg of Bi) (g of HAP)$^{-1}$.

The purpose of this work is to reveal specific features of the interaction of bismuth(III) with HAP of various morphologies for the sorption and co-crystallization binding methods. The ability of HAP to co-crystallization binding of the bismuth complexes with AP was studied. Special attention was given to the possibility of formation of the intrinsic phase by bismuth in this process.

Experimental

Morphological types of hydroxyapatite. Several morphological types of HAP were chosen for the sorption binding processes: hydroxyapatite synthesized according to a previously described[17] as a powder (HAP-0), HAP_T obtained similarly but subjected to the thermal treatment,[18] and HAP_E (E is enzyme) formed during alkaline hydrolysis of calcium glycerophosphate using alkaline phosphatase.[19]

Synthesis of HAP-0 was described in detail.[20,21] This hydroxyapatite had average particle sizes of 125±20 μm and was prepared from an aqueous suspension of nanoparticles by drying at 80 °C to a constant weight and selecting the fraction of particles with the necessary size. The specific surface area was determined by the thermal desorption of nitrogen on a Micrometrics ASAP 2010M instrument (USA) with result processing *via* the Brunauer—Emmett—Teller (BET) method (analysis was performed at $T = 77$ K and relative vapor pressure $P/P_0 = 0.2$). The specific surface area was 70±10 m^2 g^{-1}.

HAP_T was obtained by the thermal treatment of HAP-0 in a MIMP furnace (Russia) at 1200 °C for 3 h. Its specific surface was 40±5 m^2 g^{-1}.

HAP_E prepared according to a previously published procedure[19] represented hollow solid spherical hydroxyapatite particles with an average diameter of 2.7 μm and a specific surface area of 180 m^2 g^{-1}.

Co-crystallization introduction of bismuth ions into the reaction mixture for the synthesis of HAP was carried out according to a described procedure[22] using an aqueous solution of bismuth nitrate, which was prepared by the dissolution of a weighed sample of $Bi(NO_3)_3 \cdot 5H_2O$ in distilled water with stirring and adding a minimum amount of HNO_3 (0.1 mol L^{-1}). The amount of the introduced salt was chosen in such a way that the weight of bismuth would be 5% of the HAP weight. Three samples of the suspensions were synthesized: HAP-Bi_1 (content of the solid phase X_s = 4.05 wt.%), HAP-Bi_2 (X_s = 3.95 wt.%), and HAP-Bi_3 (X_s = 3.73 wt.%). Aliquots of the experimental suspensions were sampled for the subsequent morphological analysis. After the synthesis, samples of the mother liquors were separated from the solid phase by centrifuging. The residual contents of bismuth and calcium ions in solution (and AP in the case of using the complexes) were determined spectrophotometrically. The solid phase was dried to a constant weight at 80 °C for the subsequent study of its phase composition.

Chemical analysis of solutions to the content of bismuth and calcium ions was conducted by spectrophotometry on a Shimadzu UV-1280 instrument (Japan, measurement increment 1 nm). The Bi^{3+} content was determined using a solution of ethylenediaminetetraacetic acid (EDTA),[23] which forms the $[Bi(EDTA)]^-$ complex with the absorption wavelength 265 nm. It has previously been shown that the complex formed by calcium ions does not impede the determination of bismuth. The calcium concentration was determined in experiments using the Kal′tsium-KFK analytical set (Agat, Russia) at λ = 575 nm by the procedure recommended by the producer. The concentration of the 2-aminopyrimidine ligand was determined spectrophotometrically using the calibration by the absorption wavelengths of the complex 224 and 291 nm.

Phase composition of the studied samples was monitored with a DRON-3 automated X-ray diffractometer focused according to the Bragg—Bretano geometry with a graphite monochromator on the diffracted beam controlled using the EXPRESS computer program. The measurements were conducted with a Co-Kα X-ray tube (radiation wavelength 0.179021 nm, stepwise scan mode in the angle range 2θ = 10—80° with an increment of 0.1—0.05°). The exposure time per one point was 3—5 s.

Morphology of samples was examined by transmission electron microscopy (TEM, JEM-1011B microscope, Japan, resolution 0.3 nm). Some samples were studied using high-resolution transmission electron microscopy (HR-TEM) on a Jeol JEM-2100 F microscope (Japan) with the possibility of energy dispersive X-ray microanalysis (EDX).

Kinetics of bismuth sorption on HAP-0, HAP_T, and HAP_E. A 0.1 *M* solution of $Bi(NO_3)_3$ (5 mL), distilled water (5 mL), and HAP-0 powder (50 mg) were mixed in six 10-mL plastic tubes. The contents of the tubes were stirred with a Multi Bio RS-24 programmed rotator (Latvia). The stirring duration was varied from 1 to 120 min. After the necessary time period, a suspension was centrifuged for 5 min (MLW T.51.1 centrifuge, 3000*g*, German Democratic Republic). The contents of bismuth and calcium were determined as described above in an aliquot of the mother liquor, as well as the contents of the ligands (complexes). Experiments on the HAP_T and HAP_E samples were performed similarly.

The experiment on establishing a dependence of the pH of a HAP suspension on the sorption duration of Bi^{3+} ions was additionally conducted. For this purpose, a suspension of HAP-0 was added to solutions of bismuth of a certain concentration. The resulting mixture was magnetically stirred (MLW-RH3 magnetic stirrer, German Democratic Republic), and a change in the pH of the mixture was recorded during the whole experiment (ELIT 3305 pH-meter, England). In the first case (with the minimum bismuth concentration), distilled water (40 mL), a Bi solution (50 mL, 39.5 mg mL^{-1}), and a suspension of HAP-0 (10 mL) were mixed. The Bi concentration was 20 mg mL^{-1}. In

the second case (with the maximum bismuth concentration), a solution of Bi (90 mL, 118.5 mg mL^{-1}) and a suspension of HAP-0 (10 mL). The Bi concentration was 106.6 mg mL^{-1}.

Sorption isotherm was obtained using the following concentrations of a $Bi(NO_3)_3$ solution: 20, 30, 40, 60, 80, 100, and 120 mg mL^{-1}. The HAP powder (HAP-0, HAP_T, or HAP_E) (50 mg) was loaded to seven 10-mL plastic tubes, a solution of bismuth(III) nitrate (10 mL) with chosen concentrations was added, and the mixtures were stirred for 30 min (the time was determined from the sorption kinetics data). The phases were separated by centrifugation, aliquots of the liquid fraction were sampled, and the bismuth content was determined in them according to a procedure described above.

Results and Discussion

As can be seen from Fig. 1, bismuth is rapidly sorbed on all presented types of HAP, and the differences correspond to a change in the specific surface areas of the HAP samples. The obtained sorption isotherms (Fig. 2) nearly coincide with each other regardless of the type of HAP used and cannot be described in terms of the Langmuir or Freundlich models. This is related, most likely, to the formation of the intrinsic phase of bismuth during sorption. Taking into account the data obtained, we can assume that some "jump" at a certain bismuth concentration is related to the formation of such a phase, the formation of which induces an additional sorption of bismuth on it. This is especially noticeable for the HAP_E sample, probably, due to its higher specific surface area.

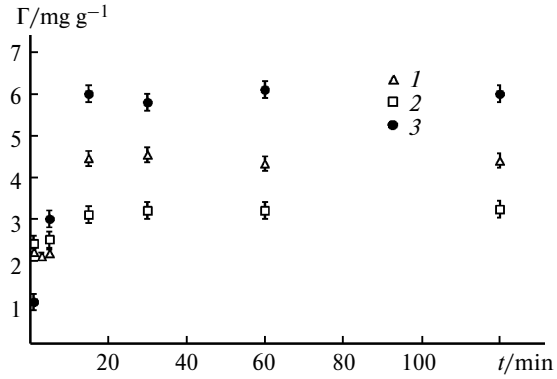

Fig. 1. Sorption kinetics of bismuth(III) ions on particles of HAP-0 (*1*), HAP_T (*2*), and HAP_E (*3*). The specific surface area of the samples is 70, 40, and 180 $m^2\ g^{-1}$, respectively.

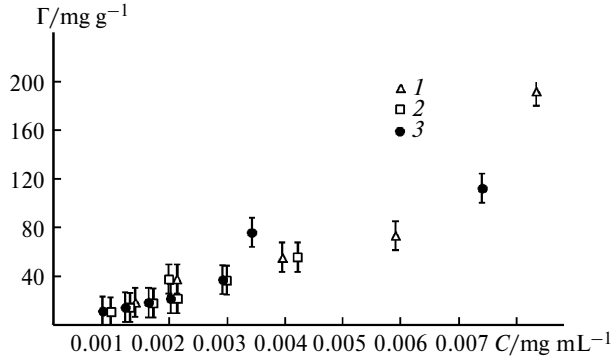

Fig. 2. Sorption isotherms of bismuth(III) ions on particles of HAP-0 (*1*), HAP_T (*2*), and HAP_E (*3*).

For co-crystallization binding of HAP with bismuth ions, the obtained diffraction patterns do not indicate the formation of the intrinsic phase of bismuth, as well as the TEM data (Fig. 3). However, microscopy reveals some difference in crystal sizes, indicating the morphological changes related to the formation of amorphized particles. This fact is indicated by a decrease in the intensity and broadening of the main peaks in the diffraction patterns of the experimental samples.

The change in the sizes related to amorphization (together with other factors) is shown in Fig. 4, where the distribution functions of the particles over length and width are presented. It is seen that bismuth ions exert the highest effect on the morphology of the HAP particles in the case of their introduction at the beginning of the synthesis ($HAP\text{-}Bi_1$). The particles with the sizes substantially smaller than those of pure HAP are formed. In the cases of the $HAP\text{-}Bi_2$ and $HAP\text{-}Bi_3$ samples, the length of the nanocrystals increases and their width decreases. The average sizes of the experimentally obtained crystals are presented in Table 1. Neither X-ray diffraction analysis, nor HR-TEM detects bismuth particles forming the intrinsic phase. The data of local EDX analysis indicate almost no bismuth on the surface of the HAP particles. However, some particles, which can aspire to play the role of the intrinsic phase of bismuth, are observed on the TEM images (Fig. 5). The results of chemical results of the mother liquor of suspensions of $HAP\text{-}Bi_1$, $HAP\text{-}Bi_2$, and $HAP\text{-}Bi_3$ showed that the residual concentration of Ca^{2+} in them was $(6.86\pm0.05)\cdot10^{-2}$, $(4.49\pm0.05)\cdot10^{-2}$, and $(4.19\pm0.05)\cdot10^{-2}$ mol L^{-1}, respectively, and the residual concentration of Bi^{3+} ions was $(2.91\pm0.19)\cdot10^{-5}$, $(1.85\pm0.12)\cdot10^{-5}$, and $(1.75\pm0.12)\cdot10^{-5}$ mol L^{-1}. It follows from the data presented that the composition of the solid phase corresponds to the empirical formula $Ca_9Bi(PO_4)_6(OH)_2$. However, this does not correspond to the real phase composition.

Table 1. Average sizes (length and width) of HAP-Bi nanocrystals obtained by the co-crystallization method

Sample	Average length	Average width
	nm	
HAP-0	103±10	35±3
$HAP\text{-}Bi_1$	26.6±3.0	6.4±0.7
$HAP\text{-}Bi_2$	131±10	29±3
$HAP\text{-}Bi_3$	127±10	27±3

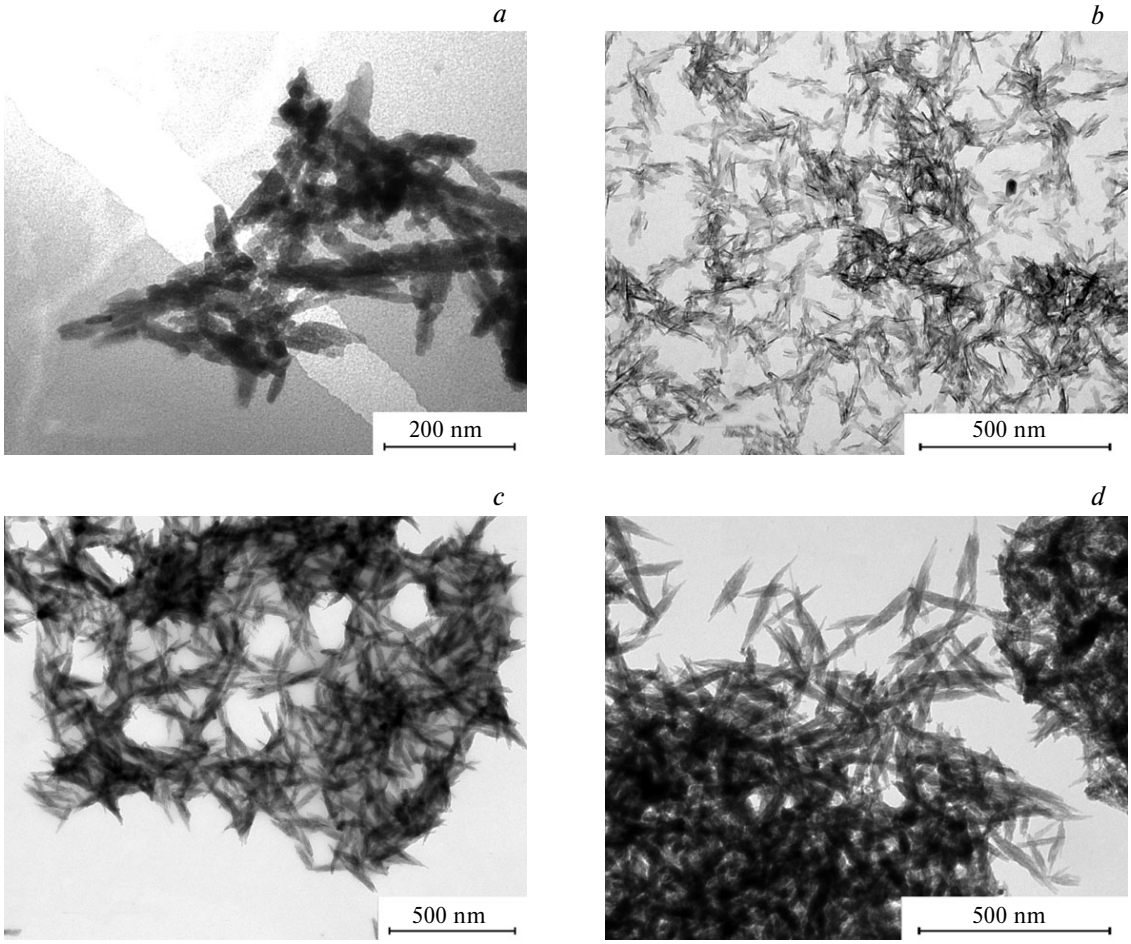

Fig. 3. TEM data for samples of HAP-0 (*a*), HAP-Bi_1 (*b*), HAP-Bi_2 (*c*), and HAP-Bi_3 (*d*).

The experiment on establishing the dependence of the pH of a suspension of HAP on the sorption duration of Bi^{3+} ions showed that for a minimum bismuth concentration of 20 mg mL^{-1} the pH was 0.2 and remained unchanged for 1.5 h. At the maximum bismuth concentration equal to 106.6 mg mL^{-1}, the pH was 0.4 within this time. This fact asserts that at such a low pH HAP cannot exist for a long time and will either dissolve or transit to more acidic forms of calcium phosphates. Therefore, in spite of the data[16] describing a similar process at somewhat higher

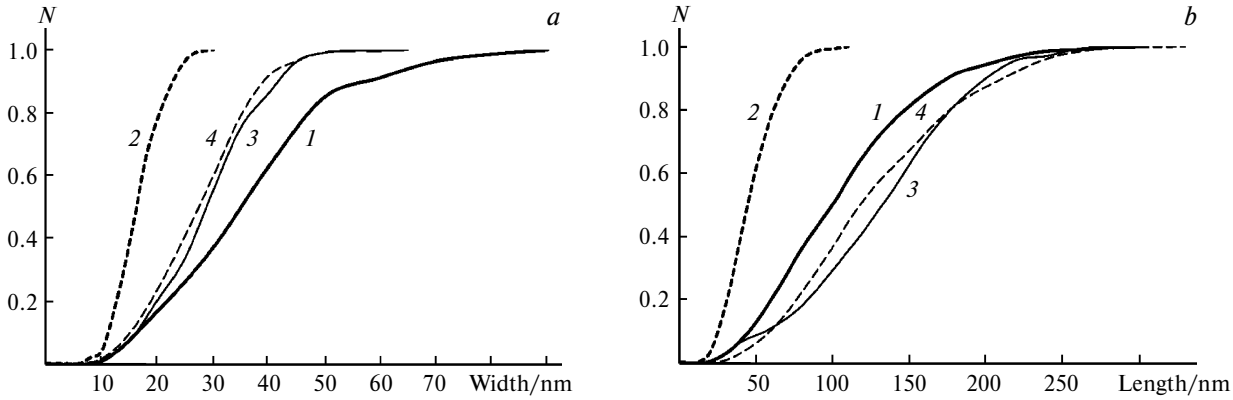

Fig. 4. Distribution functions for nanocrystals of HAP-Bi compared to HAP-0 over width (*a*) and length (*b*): HAP-0 (*1*), HAP-Bi_1 (*2*), HAP-Bi_2 (*3*), and HAP-Bi_3 (*4*).

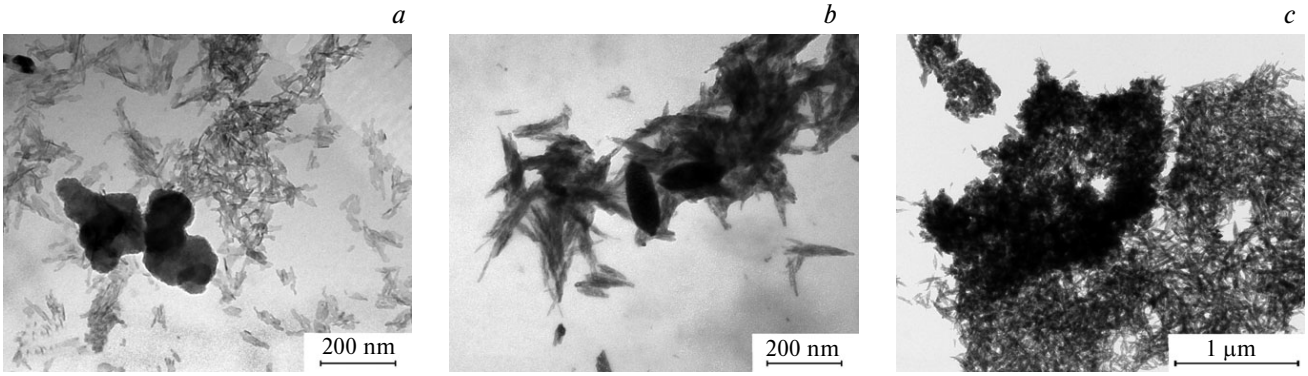

Fig. 5. TEM images of particles of the foreign phase in samples of HAP-Bi_1 (*a*), HAP-Bi_2 (*b*), and HAP-Bi_3 (*c*).

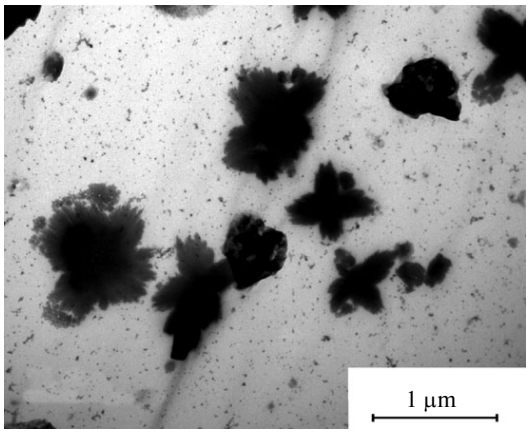

Fig. 6. TEM images of particles of bismuth phosphate formed after the adsorption of the maximum (106.6 mg mL^{-1}) amount of bismuth on HAP-0.

pH values (~1—2) as sorption, we believe that the chemical (through a solution) or topochemical (on the surface of the HAP nanoparticles) reaction of formation of bismuth phosphate with a very low solubility (solubility product ~10^{-20}) in the form of an intrinsic solid phase. This is confirmed by the results of the TEM studies of the suspension samples after the sorption experiments, which distinctly demonstrate the formation of the foreign phase of bismuth phosphate (Fig. 6). The X-ray diffraction data for the considered samples (Fig. 7) unambiguously confirm the advanced assumption, and almost no lines of the HAP itself are observed (or they are disguised by the intense lines of bismuth phosphate).

An attempt to introduce bismuth as complexes with 2-aminopyrimidine cation into the co-crystallization or sorption interaction failed, since these complexes turned out to be insufficiently stable in weakly acidic and neutral aqueous and physiological solutions. They rapidly undergo hydrolysis to form poorly soluble hydroxo complexes or bismuth hydroxide.

Thus, it is unreasonable to introduce bismuth into HAP using the direct sorption and co-crystallization method at relatively high concentrations of the latter. Alternative

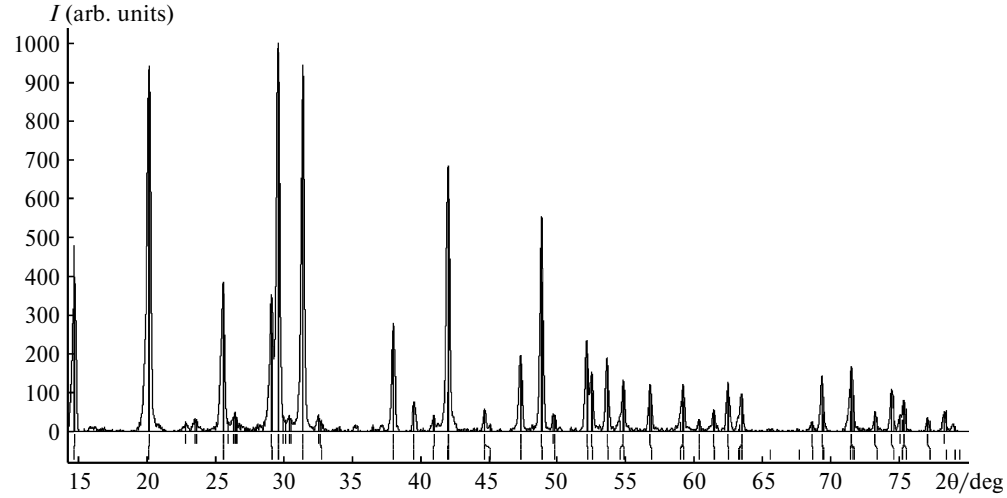

Fig. 7. Diffraction pattern of samples of the solid phase obtained after bismuth sorption on HAP-0. Reference reflections for bismuth phosphate are presented by dashes for comparison.

approaches are needed for the combined use of bismuth ions or its complexes and HAP. Among these approaches, the use of albumin as a spacer capable of retaining the HAP-Bi—AP system as a single whole seems to be very promising.

This work was financially supported by the Russian Foundation for Basic Research (Project Nos 18-03-00432 and 19-08-00055) using the equipment of the Scientific Research and Educational Center for Collective Use "Nanochemistry and Nanomaterials."

References

1. V. A. Semenov, Yu. Yu. Rusakov, D. O. Samultsev, L. B. Krivdin, *Mendeleev Commun*., 2019, **29**, 315.
2. Y. Kondo, M. Satoh, N. Imura, M. Akimoto, *Anticancer Res.,* 1992, **12**, 2303.
3. T. L. Rosenblat, M. R. McDevitt, D. A. Mulford, N. Pandit Taskar, C. R. Divqi, K. S. Panageas, M. L. Htaney, S. Morgenstem, A. Sgouros, S. M. Larson, D. A. Scheinberg, J. G. Jurcic, *Clin. Cancer Res.,* 2010, **16**, 5303.
4. B. I. Egorova, O. A. Fedorova, S. N. Kalmykov, *Russ. Chem. Rev*., 2019, **88**, 901.
5. P. J. Sadler, H. Li, H. Sun, *Coord. Chem. Rev.,* 1999, **185—186**, 689.
6. W. Frank, G. J. Reiss, J. Schneider, *Angew. Chem.*, 1995, **34**, 2416.
7. A. S. Rao, U. Baruah, S. K. Das, *Inorg. Chim. Acta*, 2011, **372**, 206.
8. S. A. Adonin, M. N. Sokolov, V. P. Fedin, *Coord. Chem. Rev*., 2016, **312**, 1.
9. V. Yu. Kotov, A. B. Ilyukhin, P. A. Buikin, K. E. Yorov, *Mendeleev Commun.,* 2019, **29**, 537.
10. T. P. Trofimova, M. A. Orlova, V. A. Tafeenko, A. N. Proshin, I. S. Glazkova, D. A. Pankratov, *Mendeleev Commun*., 2019, **30**, 2335.
11. S. Markovic, L. Veselinovic, M. J. Lukic, L. Karanovic, I. Bracko, N. Ignjatovic, D. Uskokovic, *Biomed. Mater.*, 2011, **6**, 045005.
12. M. K. Ahmed, S. F. Mansour, M. S. Mostafa, R. Darwesh, S. I. El-dek, *J. Mater. Sci*., 2019, **54**, 1977.
13. J. H. Shepherd, D. V. Shepherd, S. M. Best, *J. Mater. Sci. Mater. Med*., 2012, **23**, 2335.
14. T. J. Webster, E. A. Massa-Schlueter, J. L. Smith, E. B. Slamovich, *Biomaterials*, 2004, **25**, 2111.
15. D. Govindaraj, C. Govindasamy, M. Rajan, *Mater. Sci. Engineer. C*, 2017, **79**, 875—885.
16. S. Zamani, E. Salahi, I. Mobasherpour, *Res. Chem. Intermed*., 2014, **40**, 1753.
17. I. V. Melikhov, V. F. Komarov, A. V. Severin, V. E. Bozhevol´nov, V. N. Rudin, *Dokl. Akad. Nauk*, 2000, **373**, 355 [*Dokl. Chem.* (*Engl. Transl.*), 2000] (in Russian).
18. E. I. Suvorova, V. V. Klechkovskaya, V. F. Komarov, A. V. Severin, V. N. Rudin, *Crystallogr. Rep.*, 2006, **51**, 881.
19. M. A. Orlova, A. L. Nikolaev, T. P. Trofimova, A. P. Orlov, A. V. Severin, S. N. Kalmykov, *Vestn. RGMU*, 2018, No. 6, 94 [*Bull. RSMU* (*Engl. Transl.*), 2018, No. 6, 86] (in Russian).
20. A. V. Severin, M. A. Orlova, E. S. Shalamova, T. P. Trofimova, I. A. Ivanov, *Russ. Chem. Bull.*, 2017, **66**, 9.
21. M. A. Orlova, A. L. Nikolaev, T. P. Trofimova, A. V. Severin, A. V. Gopin, N. S. Zolotova, V. K. Dolgova, A. P. Orlov, *Russ. Chem. Bull*., 2019, **68**, 1102.
22. A. V. Severin, D. A. Pankratov, *Zh. Neorg. Khim*., 2016, **61**, 279 [*Russ. J. Inorg. Chem*. (*Engl. Transl*.), 2016, **61**] (in Russian).
23. V. B. Aleskovskii, *Fiziko-khimicheskie metody analiza* [*Physico-chemical Analysis Methods*], Ripol Klassik, Moscow, 2013, 116 (in Russian).

Received November 28, 2019;
in revised form January 28, 2020;
accepted February 4, 2020